HHS Public Access

Author manuscript

Methods Enzymol. Author manuscript; available in PMC 2019 September 25.

Published in final edited form as:

Methods Enzymol. 2018 ; 611: 559–582. doi:10.1016/bs.mie.2018.08.014.

A Tethered Vesicle Assay for High-Throughput Quantification of Membrane Fission

Wilton T. Snead[*] and **Jeanne C. Stachowiak**[*,†,1]

[*]Department of Biomedical Engineering, The University of Texas at Austin, Austin, TX, United States

[†]Institute for Cellular and Molecular Biology, The University of Texas at Austin, Austin, TX, United States

Abstract

Membrane fission, which divides membrane surfaces into separate compartments, is essential to diverse cellular processes including membrane trafficking and cell division. Quantitative assays are needed to elucidate the physical mechanisms by which proteins drive membrane fission. Toward this goal, several experimental tools have been developed, including visualizing fission products using electron microscopy, measuring membrane shedding from a lipid reservoir, and observing fission of individual membrane tubes pulled from giant vesicles. However, no existing assay of membrane fission provides a quantitative, high-throughput measure of the distribution of vesicle curvatures generated by fission-driving proteins. Toward addressing this challenge, here we describe a novel approach that uses confocal fluorescence imaging to quantify the diameter distribution of membrane vesicles that have been tethered to a coverslip surface following exposure to fission-driving proteins. We employ this assay to measure the progressive appearance of high curvature fission products upon exposure of vesicles to increasing protein concentration. Results from this approach are in quantitative agreement with measurements from electron microscopy, but can be collected with considerably greater throughput, enabling examination of a broad range of experimental conditions. Using the tethered vesicle approach, we have recently found that membrane-bound intrinsically disordered proteins are surprisingly potent drivers of membrane fission. The capacity to drive fission arises from steric pressure generated when disordered domains with large hydrodynamic radii bind to membranes at high local densities. More broadly, the experimental tools described here have the potential to improve our mechanistic understanding of membrane fission in diverse biophysical contexts.

1. INTRODUCTION

The process of membrane fission, which divides a continuous membrane surface into two or more separate compartments, is essential for cellular life (McMahon & Gallop, 2005). Cellular functions which rely on membrane fission include membrane trafficking (Conner & Schmid, 2003), cellular division (Mierzwa & Gerlich, 2014), and organelle biogenesis

[1]Corresponding author: jcstach@austin.utexas.edu.

The authors declare no conflict of interest.

(Hoppins, Lackner, & Nunnari, 2007), among others. Harmful pathogens such as viruses and bacterial toxins also require membrane fission to enter and exit cells (Hurley, Boura, Carlson, & Rozycki, 2010). Therefore, detailed characterization of the physical mechanisms that drive membrane fission is important for understanding normal cell function as well as the physiology of disease.

Membrane fission is an energetically costly process (Helfrich, 1973), which relies upon significant energetic contributions from diverse protein machines (Zimmerberg & Kozlov, 2006). Quantitative experimental tools are needed to understand how individual proteins and molecular mechanisms overcome the energetic barriers to membrane fission. A significant body of work from multiple research groups has led to the development of a variety of assays for studying membrane fission (Fig. 1). Among the most common techniques is negative stain transmission electron microscopy (TEM) of vesicles, which enables direct visualization of the fission products generated upon mixing of membrane vesicles and proteins (Boucrot et al., 2012; Ford et al., 2002) (Fig. 1A). More recently, supported bilayers with extra membrane reservoir have been developed. These “SUPER” templates consist of glass beads coated with a low-tension membrane bilayer (Neumann, Pucadyil, & Schmid, 2013; Pucadyil & Schmid, 2008). Exposure of SUPER templates to fission-driving proteins leads to quantifiable release of membrane vesicles (Fig. 1B). Finally, lipid tubules pulled from giant unilamellar vesicles (GUVs) (Prevost, Tsai, Bassereau, & Simunovic, 2017) enable simultaneous measurement of lipid tubule diameter and protein binding, providing a highly controlled setting for observing membrane fission events (Fig. 1C).

While experimental systems like negative stain TEM, SUPER templates, and GUVs have enabled the investigation of membrane fission mechanisms, these tools generally required researchers to choose between the ability to make highly quantitative measurements and the ability to examine multiple conditions with high throughput. For example, SUPER templates provide a measure of the relative extent of membrane fission, quantified as the bulk fluorescence of membrane released by the addition of proteins (Neumann et al., 2013). While these experiments can achieve high throughput, they do not quantify the diameters of the fission products. In contrast, GUV tube-pulling assays provide highly quantitative estimates of membrane curvature, but can examine only a single lipid tubule at a time (Prevost et al., 2017), greatly limiting throughput. Finally, while TEM experiments quantify the diameters of fission products, they typically rely on manual analysis of vesicles in electron micrographs (Boucrot et al., 2012). This approach greatly limits throughput and can be biased by the selection of the field of view as well as insufficient understanding and control of vesicle adsorption and staining on TEM grids (Franken, Boekema, & Stuart, 2017). In light of these limitations, the development of novel assays that provide quantitative results in a high-throughput format is needed.

Here we describe a high-throughput assay for quantifying the distributions of vesicle diameters resulting from membrane fission. This procedure uses confocal fluorescence imaging to measure the brightness of individual, immobilized fluorescent vesicles. These measurements are then converted to distributions of vesicle diameter by calibrating the measured brightness distribution against an independent measure of the distribution of vesicle diameter from dynamic light scattering (DLS) (Fig. 2). This assay builds upon earlier

work from the Stamou group (Hatzakis et al., 2009; Kunding, Mortensen, Christensen, & Stamou, 2008; Lohr, Kunding, Bhatia, & Stamou, 2009), which utilized immobilized vesicles to measure the sensitivity of proteins to membrane curvature. However, our procedure, first reported in a recent study (Snead et al., 2017), is the first to use this experimental approach for quantifying the vesicle diameter distribution created during membrane fission. We validated our procedure by comparing it to traditional negative stain TEM of vesicles. Both approaches yield similar estimates of average vesicle diameter (see Section 4). However, the tethered vesicle assay provides much more detail about the distribution of vesicle diameters with considerably less experiment time in comparison to TEM. As such, the tethered vesicle assay facilitates study of membrane fission across a broad range of experimental parameters such asprotein concentration and membrane composition. Therefore, the assay described here may be utilized to gain a more detailed understanding of how proteins drive membrane fission in a variety of biophysical contexts.

Based on studies that have employed combinations of the assays described above, the prevailing view is that membrane fission is mediated primarily by structured proteins or protein assemblies (Jarsch, Daste, & Gallop, 2016; McMahon & Gallop, 2005), including the ESCRT machinery (Schoneberg, Lee, Iwasa, & Hurley, 2017) or the dynamin helical scaffold (Antonny et al., 2016). In contrast, recent work from our group found that protein crowding can drive membrane fission independent of protein structural or assembly properties (Snead et al., 2017). Specifically, molecular crowding among proteins attached to membrane surfaces at high density generates steric pressure that can bend membranes and ultimately overcome the energetic barrier to membrane fission (Busch et al., 2015; Snead et al., 2017; Stachowiak et al., 2012). In support of this mechanism, we found that bulky, intrinsically disordered proteins, which occupy significantly larger membrane footprints in comparison to well-folded proteins of similar mass (Hofmann et al., 2012), can be potent drivers of membrane fission. Specifically, we examined membrane fission by Epsin 1, an adaptor protein of the clathrin-mediated endocytic pathway which contains a well-folded epsin N-terminal homology (ENTH) domain and a bulky, disordered domain. As shown below, both SUPER template experiments (Fig. 1B) and tethered vesicle experiments (Fig. 6) reveal that full-length Epsin 1 drives membrane fission more efficiently in comparison to the isolated ENTH domain (Snead et al., 2017).

2. TETHERED VESICLE FISSION ASSAY

In this section we describe procedures for preparing the vesicles and tethering substrates and performing the fission experiment. In the next section we describe the image analysis procedure used to quantify the distribution of vesicle diameters before and after fission. Fig. 2 shows an overall schematic of this workflow.

2.1 Preparing Vesicles

When designing a vesicle composition for fission studies, the lipid components should be chosen to adequately represent the membrane environment of interest. Factors to consider when designing a membrane composition include the binding lipid for the protein, the membrane bending rigidity, and the net charge of the membrane, among others. The lipid

components can be adjusted to capture a variety of membrane physical and chemical properties.

In the experiments described here, we examine membrane fission by the ENTH domain of the clathrin adaptor protein Epsin 1. ENTH binds preferentially to the lipid phosphatidylinositol-4,5-bisphosphate (PIP_2), and inserts an N-terminal, amphipathic helix into the membrane surface (Ford et al., 2002). To study membrane fission by the ENTH domain, we use membranes composed primarily of 1,2-dioleoyl-*sn*-glycero-3phosphocholine (DOPC). PIP_2 is incorporated to facilitate ENTH binding, as well as the negatively charged lipid 1,2-dioleoyl-*sn*-glycero-3-phosphoL-serine (DOPS) to further enhance ENTH recruitment via electrostatic interactions. The fluorescently labeled lipid Oregon Green 488 1,2dihexadecanoyl-*sn*-glycero-3-phosphoethanolamine (Oregon Green 488DHPE) is included to enable vesicle imaging, and the biotinylated lipid dipalmitoyl-decaethylene glycol-biotin (DP-EG10-biotin (Momin et al., 2015)) enables vesicle tethering. While the procedures described here focus on the ENTH domain, the membrane composition can readily be adapted to examine a wide variety of fission-driving proteins that bind to membrane surfaces.

2.1.1 Equipment

- Glass syringes for mixing lipids in solvent (Hamilton)
- Rotary evaporator (optional)
- Nitrogen gas
- Vacuum chamber and pump
- Mini extruder system (Avanti Polar Lipids, Alabaster, AL)

2.1.2 Reagents

- Lipids: PIP_2, DOPC, and DOPS (Avanti). PEG-biotin lipid (we use a custom-synthesized DP-EG10-biotin lipid (Momin et al., 2015), but others are available from Avanti). Fluorescent lipid (Oregon Green 488-DHPE; Thermo Fisher)
- Chloroform, methanol, ultrapure water
- MOPS, HEPES, NaCl, EDTA, EGTA (Sigma or Fisher)

2.1.3 Procedure

1. The lipid composition for experiments with ENTH is: 77.5mol% DOPC, 15mol % DOPS, 5mol% PIP_2, 0.5mol% Oregon Green 488DHPE, and 2mol% DP-EG10-biotin. In a clean glass conical tube, mix lipids in chloroform at the specified molar ratios.
    a. When working with PIP_2, the solvent mixture must be adjusted with methanol and water prior to adding PIP_2 such that the volume ratio is 20:9:1 chloroform:methanol:water, to ensure that PIP_2 remains soluble.

2. Dry the lipid into a film via rotary evaporation or under a stream of nitrogen. Dry further under vacuum for at least 2h, preferably overnight.
3. Hydrate the lipid film in experiment buffer of 20m*M* MOPS or 25m*M* HEPES pH 7.35 and 150m*M* NaCl. Vortex well.
4. Extrude using a 200nm pore membrane in a mini extruder system.

2.1.4 Notes

- If needed, colorimetric assays for quantifying phospholipid concentration may be used after preparing the vesicles (Stewart, 1980; Takayama, Itoh, Nagasaki, & Tanimizu, 1977). The phosphatidylcholine assay described in Takayama et al. is available as a kit from several vendors.
- Store vesicles at 4°C and use within 48h, as PIP_2 will degrade. Vesicles without PIP_2 can be stored for up to a week before degradation becomes a concern.
- Include 0.5m*M* EDTA and EGTA in the buffer to prevent clustering of PIP_2 by divalent metal cations (Ellenbroek et al., 2011), which are present as trace contaminants in most buffers and salts.
- Our previous work has also utilized the synthetic lipid 1,2-dioleoyl-*sn*-glycero-3-[(*N*-(5-amino-1-carboxypentyl)iminodiacetic acid)succinyl], nickel salt (DOGS-NTA-Ni) in order to examine membrane fission by hexahistidine (6his)-tagged proteins. For example, our recent work showed that membrane-bound green fluorescent protein drove fission when recruited to DOGS-NTA-Ni membranes by a 6his tag (Snead et al., 2017). In these experiments, PIP_2 and DOPS are replaced with 20mol% DOGS-NTA-Ni. EDTA and EGTA should not be used in the buffer here, as they will bind and sequester nickel ions needed to promote 6his–NTA interactions.

2.2 Preparing Tethering Substrates

In order to tether the vesicles to a coverslip surface for imaging, the surface must first be passivated and functionalized with biotin. Here we use PEG and PEG-biotin for passivating the glass. Once passivated, the biotinylated vesicles are tethered to the PEG-biotin molecules by binding to neutravidin (see Section 2.2.6). Glass passivation can be achieved in two ways: (1) coating the glass with poly-L-lysine (PLL) conjugated to PEG and PEG-biotin, or (2) directly conjugating PEG and PEG-biotin to the glass via silanization. Here we describe procedures for cleaning and passivating glass using both of these approaches.

2.2.1 Equipment

- Glass coverslips, 24×40mm (VWR cat. no. 48393–230)
- Glass carafes with slots for individual coverslips
- Glove bag
- Clean oven (for drying coverslips and performing the silane reaction)
- Princeton CentriSpin-20 size exclusion spin columns (Princeton Separations)

- Silicone gaskets
  - To make gaskets, we purchase 0.8-mm-thick silicone sheets (Grace Bio-Labs cat. no. 664172), cut out small pieces, and punch holes for imaging wells using a 0.5mm biopsy punch. The wells hold approximately 40μL.

2.2.2 Reagents

- RCA glass cleaning: 100% ethanol, ultrapure water, 30% H_2O_2, KOH, 37% HCl (Sigma or Fisher)
- PLL (Sigma)
- For PLL-PEG-biotin: mPEG-SVA (mPEG-succinimidyl valerate) and biotin-PEG-SVA (both having PEG chains of 5000Da; Laysan Bio, Arab, AL)
- For silanization reaction: mPEG-silane and biotin-PEG-silane (both having PEG chains of 5000Da; Laysan Bio)
- Sodium tetraborate (Fisher)
- Anhydrous isopropanol (Fisher)
- Glacial acetic acid (Fisher)
- Neutravidin (Thermo Fisher cat. no. 31000)
  - We purchase lyophilized neutravidin powder, create a 1mg/mL solution in PBS or 25m*M* HEPES pH 7.35, 150m*M* NaCl, and store aliquots at –80°C.

2.2.3 RCA Glass Cleaning

Precautions: Appropriate personal protective equipment must be used when performing RCA glass cleaning, including chemical gloves, apron, and face shield. The procedure must be performed in a chemical fume hood, as the acid and base solutions with hydrogen peroxide generate caustic fumes. Prepare the acid and base solutions separately, and do not mix them together. Dilute the HCl by slowly pouring the concentrated HCl into water. Do not add water directly to concentrated HCl.

1. Place coverslips in carafes and add 100% ethanol to cover. Sonicate in a bath sonicator for 10min. Rinse thoroughly with ultrapure water to remove all ethanol.
2. In a separate beaker, prepare a solution of 1.5 *M*KOH in ultrapure water and heat to 70–80°C. Slowly add H_2O_2 to a final concentration of 7.5% and stir well. Bubbles will appear spontaneously as the solution reacts. Pour the reactive mixture into the carafes to cover the slides. Let stand for 10min and then rinse the carafe thoroughly with ultrapure water until all reactants are removed.
3. In a separate beaker, prepare a solution of 2.4 *M* HCl in ultrapure water and heat to 70–80°C. Slowly add H_2O_2 to a final concentration of 6.3% and stir well. Bubbles will appear spontaneously as the solution reacts. Pour the reactive

mixture into the carafes to cover the slides. Let stand for 10min and then rinse the carafe thoroughly with ultrapure water until all reactants are removed. Store clean slides in ultrapure water and use them within 2 weeks.

2.2.4 Preparing PLL-PEG-Biotin

1. Dissolve PLL at a concentration of 40mg/mL in 50m*M* sodium tetraborate at pH 8.5.
2. Calculate the amount of PEG-SVA needed to achieve a molar ratio of one PEG-SVA per five lysine subunits. Include biotin-PEG-SVA at a ratio of 1:50–1:20 with PEG-SVA (2%–5% biotinylated PEG).
3. In a glove bag filled with nitrogen gas, measure out PEG-SVA and biotin-PEG-SVA powders. Close and seal stock containers in the glove bag, as the PEGs are hygroscopic and should be stored in a low moisture environment.
    a. We like to pour out more of the PEG powder than needed in the glove bag, and then take the powder out of the glove bag and precisely measure the desired amount using a scale. Discard the excess powder that is not used. Once the powders are taken out of the glove bag, work quickly to weigh the powders and proceed to the reaction step.
4. Combine the PEG powders and mix well.
5. Add the PLL solution to the amine-reactive PEG-SVA powder, vortex well, and transfer to a test tube with a small stir bar. Stir continuously for 6h at room temperature.
6. Separate PLL-PEG-biotin from the unconjugated molecules using CentriSpin-20 size exclusion spin columns hydrated with PBS or 25m*M* HEPES pH 7.35 and 150m*M* NaCl. Store at 4°C until use.

2.2.5 Passivating Glass With PEG-Silane

1. Dry ultraclean coverslips under a stream of nitrogen and further dry in a clean oven at 70–100°C for at least 30min.
2. Create a 0.67% solution of PEG-silane in anhydrous isopropanol, with biotin-PEG-silane comprising 2%–5% of the total PEG amount, as described above. Sonicate in a bath sonicator for 10–15min to further dissolve the powder.
3. Add acetic acid to a final concentration of 1%.
4. Immerse the dry, ultraclean coverslips in the reactive PEG-silane solution.
5. Incubate at 70°C for 30–60min.
6. Remove the coverslips from the solution, rinse them well with ultrapure water, dry them under a stream of nitrogen, and store them dry until use.

2.2.6 Preparing Wells for Vesicle Tethering—This procedure is performed while vesicle and protein samples are incubating (see next section).

1. Place a silicone gasket, with a well volume of approximately 40μL, onto an ultraclean coverslip or silane-PEG-biotin-coated coverslip.
2. If using a silane-PEG-biotin-coated coverslip, hydrate the substrate with 20μL of buffer for approximately 5min.
3. If using an uncoated ultraclean coverslip, add 20μL of PLL-PEG-biotin solution diluted 10-fold in the experiment buffer of 20m*M* MOPS pH 7.35, 150m*M* NaCl. Coat the well for at least 20min at room temperature. Longer times of up to 60min are preferable to ensure complete coating.
4. Thoroughly wash to remove excess PLL-PEG-biotin by adding 80μL of experiment buffer to the well, removing, and discarding. Repeat at least six times.
    a. While the final volume in the well will be 40μL prior to imaging, the well can hold up to 100μL, thereby allowing for 80μL of wash buffer to be added to 20μL in the well.
5. Add 1mg/mL neutravidin solution to the well for a final concentration of approximately 0.2mg/mL. Mix well and incubate for 10min to provide sufficient time for neutravidin to bind to the biotin on the coverslip surface. Wash thoroughly with 20m*M* MOPS pH 7.35, 150m*M* NaCl following a similar procedure described in step 4.
    a. To ensure that the volume in the well remains 20μL, add the neutravidin solution to the well, mix thoroughly, and remove the same volume that was added.
    b. After washing, the well volume should be 20μL. Adding 20μL of vesicle and protein sample to the well will bring the final volume to 40μL (see Section 2.3).

The well is now ready for vesicle tethering (see Section 2.3).

2.2.7 Notes—Silicone gaskets can be cleaned and reused multiple times. Clean the gaskets by stirring them in a solution of 1–2 vol% Hellmanex detergent in ultrapure water at approximately 70–100°C for at least 15min. Following exposure to detergent, wash the gaskets thoroughly in ultrapure water and dry them well under a stream of nitrogen gas before using.

2.3 Fission Reaction and Vesicle Tethering

2.3.1 Equipment and Reagents

- Low-adhesion microcentrifuge tubes (USA Scientific cat. no. 1415–2600)
- Water bath at 37°C
- Purified membrane-binding proteins
- Vesicles (prepared in Section 2.1)

- Coverslip ready for tethering (prepared in Section 2.2)
- Experiment buffer: 20m*M* MOPS pH 7.35, 150m*M* NaCl

2.3.2 Procedure

1. Create a 20μL solution of vesicles and protein with a total lipid concentration of 10μ*M* in a low-adhesion tube. The protein concentration can vary as determined by the experimental goals. Typically, a range of protein concentrations should be tested spanning from the nanomolar to micromolar range to determine the concentration that corresponds to the onset of membrane fission.
2. Incubate the solution of vesicles and protein at 37°C for 30–60min to allow the fission reaction to take place. We chose 60min for experiments with ENTH to ensure that the fission reaction had reached completion.
3. During incubation, prepare the imaging substrate as described in Section 2.2.
4. After the fission reaction, add the 20μL solution of vesicles and protein to the imaging substrate and mix well by pipetting up and down gently several times. Wait 10min for vesicles to reach the substrate surface and become tethered.
    a. Adding 20μL of sample to the 20μL already in the well (see Section 2.2) will bring the volume to 40μL.
5. Wash to remove untethered vesicles by first removing 20μL from the well, then pipetting in 80μL of experiment buffer, removing, and discarding. Repeat at least six times. After washing, add 20μL of experiment buffer to the well to bring the well volume back to 40μL.

2.3.3 Notes

- Cover the wells with a Petri dish during incubations to avoid sample evaporation.
- Do not touch the pipet tip to the coverslip surface during washing steps.
- Image within 30min to avoid vesicle unbinding or rupturing on the substrate.

2.4 Imaging Tethered Vesicles

Image the tethered vesicles using a confocal microscope. Confocal microscopy helps to minimize the background fluorescence from untethered vesicles in solution. Wide field and TIRF microscopy may also be used, as described in protocols from the Stamou group (Kunding et al., 2008), though we only utilize confocal microscopy in this procedure. We use a spinning disc confocal microscope (Zeiss Axio Observer Z1 with Yokogawa CSU-X1M), with a 488nm excitation laser and emission filter centered at 525nm with a 50nm width. The objective is a Plan-Apochromat 100 ×, 1.4 numerical aperture (NA) oil immersion objective. Images are collected on a cooled (–70°C) EMCCD iXon3 897 camera (Andor Technology; Belfast, UK).

Acquire *z*-stacks (i.e., image stacks spaced at fixed perpendicular distances above and below the coverslip surface) that begin below the brightest, in-focus frame and extend a few frames

above the brightest frame, with a spacing of 0.1μm between frames. Acquire *z*-stacks of at least 10 fields of view within each sample to ensure an adequate number of vesicles are imaged. If possible, use the same imaging settings for all samples. For the protein-free sample, we detect approximately 200 vesicles per frame that are suitable for analysis (see next section for acceptable puncta criteria). Therefore, 10 *z*-stacks should yield approximately 2000 vesicles. The number of vesicles per frame in samples with protein may deviate from the protein-free condition, as proteins may coat the substrate and hinder vesicle tethering to some degree. Collect more than 10 *z*-stacks if the number of tethered vesicles is visibly lower than in the protein-free sample. If there are large differences in vesicle brightness between samples, for example, before and after membrane fission, parameters such as camera exposure time may need to be adjusted to improve signal quality. A linear correction for exposure time can be applied during analysis.

3. PARTICLE DETECTION AND QUANTIFICATION OF VESICLE DIAMETERS

Here, particle detection software is used to fit 2D Gaussian profiles to the diffraction-limited puncta generated in fluorescence images by individual tethered vesicles. The integrated intensities of the vesicles are proportional to the amplitudes of the Gaussian fits above the local background. These integrated intensities are also proportional to the surface areas of the vesicles. Therefore, the amplitudes of the Gaussian fits can be used to measure the relative differences in surface area among tethered vesicles. We perform particle detection using cmeAnalysis software, which was developed by the Danuser and Schmid groups to detect low signal-to-noise puncta of proteins associated with clathrin-coated endocytic structures (Aguet, Antonescu, Mettlen, Schmid, & Danuser, 2013). The software can be downloaded from the Danuser lab website. Carefully read the accompanying user guide to become familiar with how to organize data and use the software.

After detecting puncta, the distributions of vesicle brightness are converted to distributions of vesicle diameter by calibrating against an independent measurement of vesicle diameter. Specifically, we scale the median brightness value of the protein-free vesicles against the intensityweighted average diameter of the same vesicles measured by DLS. Importantly, this scaling assumes that vesicle tethering did not alter the diameter distribution measured in DLS. This assumption was tested and shown to be valid in work from the Stamou group (Kunding et al., 2008; Lohr et al., 2009). We further verify this procedure by comparing the mean diameters determined using the tethered vesicle approach to the mean diameters assessed using electron microscopy, as described below.

3.1 Cropping Images, Selecting Best-Focus Frame, and Detecting Puncta

3.1.1 Procedure

1. To avoid variations in illumination across the image, crop the images to a central region where vesicles are uniformly illuminated. Specifically, crop the images to the central square of a 3×3 grid. Cropping can be performed in MATLAB®, using the Bio-Formats software package to import Zeiss .czi files or other file types not supported by MATLAB®.

2. Calculate the mean intensity of each frame in the stack.

3. Select the frame with the greatest mean brightest as the best-focus frame for particle detection analysis.

    a. The mean intensity of the brightest frame should be a local maximum in the *z*-stack. In other words, the frames above and below should have lower mean intensities to ensure that the chosen frame is actually the best-focus frame.

4. Save the best-focus frame in a directory labeled “ch1” within a parent directory named “Celli,” where *i* is the *z*-stack number.

    a. See the cmeAnalysis user guide for more information on data organization.

5. Save the frames above and below the best-focus frame in separate directories labeled ch2 and ch3 within the same parent directory as the best-focus frame.

    a. The best-focus frame in the ch1 directory is the “master” channel in cmeAnalysis. The frames above and below in the ch2 and ch3 directories are the “slave” channels, in which the program uses the centroids of the detected puncta to search for corresponding puncta. The search radius is three times the standard deviation of the Gaussian fit to the microscope point spread function (PSF).

6. Load the dataset for an experimental condition using the command: data¼loadConditionData. The loadConditionData script will open a user interface for selecting the directory containing the data to be analyzed.

    a. Before running analysis for the first time, enter values for the NA of the objective, total magnification (M), and physical pixel size of the camera (in m) into the “Parameters” vector in loadConditionData. The software uses these inputs (along with the fluorophore specified below in step 6d) to estimate the ideal standard deviation of the microscope PSF. If the true PSF is expected to differ significantly from the ideal case, then a direct estimate of the PSF standard deviation may be loaded, as described in the cmeAnalysis user guide.

    b. A prompt will appear in the MATLAB® command window asking for the number of channels. Type “3.”

    c. Select ch1 as the master channel and ch2 and ch3 as the slave channels.

    d. A prompt will appear asking for a fluorescent marker for each channel. Since Oregon Green 488 is not a recognized fluorophore in cmeAnalysis, type “Alexa488” for each channel.

7. Pass the data to the runDetection script for particle detection with the command: runDetection(data).

8. After running detection, a folder entitled “Detection” is saved within each ch1 directory. This folder contains a file entitled “detection_v2. mat.” Opening this file imports a structured array into MATLAB® called “frameInfo,” which contains the puncta information for its respective image.

9. The “A” values in frameInfo are the amplitudes of the Gaussian fits to each puncta, which correspond to the intensities of individual puncta that will be used for further analysis.

10. Only accept A values that are significantly above the noise threshold in all three frames. Check this criterion with the “hval_Ar” logical array within frameInfo. Puncta which have a value of 1 in hval_Ar for all three channels can be used for further analysis.

11. To further exclude puncta close to the noise threshold, only accept A values that are greater than two standard deviations of the distribution of “c” values in each image. The c values are the local background intensities of each Gaussian fit.

12. Save the A values which meet the above criteria in a spreadsheet for further analysis.

Fig. 3 shows example images of vesicles before and after exposure to the ENTH domain. Membrane fission by ENTH resulted in a clear reduction in puncta brightness. The images are shown again to the right with the detected puncta marked.

3.2 Quantifying Vesicle Diameter

The final analysis step involves converting the distribution of Gaussian amplitudes (A values) obtained in the previous section to distributions of vesicle diameter. As noted above, the A values are proportional to the integrated intensity of each vesicle, and are therefore also proportional to the surface area of each vesicle. As such, the diameter of each vesicle is proportional to the square root of its A value. The use of the distribution of A values to estimate the distribution of vesicle diameters is achieved by computing a linear scaling factor that centers the square root of the median of the distribution of the A values on the intensity-weighted average diameter measured by DLS. This scaling is performed for the initial, protein-free vesicles, yielding a constant scaling factor that is then used to convert the other populations after protein exposure.

3.2.1 Dynamic Light Scattering—

Here we perform DLS measurements of the protein-free vesicles to facilitate calibration. We use a Zetasizer Nano ZS (Malvern Instruments). Note that the vesicle concentration in DLS measurements is higher than in the tethered vesicle experiments to ensure sufficient signal. We load the vesicles at approximately $500\mu M$ into a cuvette suitable for DLS, and collect at least 14 traces for 10s each. We use the average, intensity-weighted vesicle diameter distribution from these measurements for calibration, as described next.

Note: Owing to the large sample volume and vesicle concentration required for DLS-based measurements, the use of DLS to directly measure the diameter distribution after protein-driven fission is not generally feasible. In particular, a large volume of highly concentrated

purified protein solution would be required, greatly limiting the number of experiments that could be performed.

3.2.2 Converting Vesicle Intensity Distributions to Vesicle Diameter Distributions

1. Compute a scaling factor, f, for converting A values to diameter values: $f = d/\sqrt{A_{median}}$, where d is the intensity-weighted average diameter of the initial, protein-free vesicles measured by DLS, and A_{median} is the median of the A values of the initial, protein-free vesicles.
2. Create distributions of vesicle diameter for each experimental condition by multiplying the square root of the respective A values by f.
3. Create histograms of vesicle diameter for each condition to assess shifts in diameter populations after protein exposure.

See Fig. 3 for examples of puncta intensity distributions before and after membrane fission. Converting these puncta intensity distributions to vesicle diameter distributions reveals that the ENTH domain drove the formation of a high curvature vesicle population centered near 20nm diameter.

3.2.3 Examining Membrane Fission by the ENTH Domain—Using the procedure described above, we examined membrane fission by ENTH over a range of protein concentrations (Fig. 4). Experiments revealed that with increasing protein concentration, exposure to ENTH drove a progressive reduction in vesicle diameter, arriving at a high curvature population centered near 20nm.

4. COMPARISON TO AN ELECTRON MICROSCOPY-BASEDASSAY OF MEMBRANE FISSION

To verify that the tethered vesicle approach provides consistent results with established membrane fission assays, we compared the results of the 20μM ENTH condition in Fig. 4 with the results of a TEM assay performed under similar conditions. Fig. 5A shows electron micrographs of vesicles before and after exposure to ENTH, demonstrating the appearance of high curvature fission products. Measuring the vesicle diameters in these TEM images revealed that ENTH generated a vesicle population centered near 20nm diameter not observed before protein exposure (Fig. 5B). This finding is in agreement with results from the tethered vesicle assay, in which ENTH formed populations of high curvature fission vesicles centered near 20nm (Fig. 5B). This comparison indicates that the tethered vesicle approach provides consistent results with established procedures for assessing membrane fission.

Importantly, the family of distributions determined using the tethered vesicle assay (Fig. 4) can be measured in less than 1 day, but would likely be prohibitively laborious if performed using electron microscopy. Specifically, TEM image analysis required manual measurement of individual vesicles, a process that was both time consuming and somewhat subjective, owing to the low level of contrast associated with small vesicles in TEM. Therefore, the

tethered vesicle assay facilitated the analysis of more experimental conditions compared to TEM.

5. CONCLUSIONS

Here we describe an assay for assessing membrane fission using fluorescence imaging of tethered vesicles. By quantifying the distribution of vesicle diameters after fission, this approach enables examination of progressive changes in fission efficiency as a function of experimental parameters such as protein concentration and lipid composition. We utilized this assay to demonstrate that bulky, intrinsically disordered protein domains can be potent drivers of membrane fission (Snead et al., 2017). Specifically, when we examined membrane fission by full-length Epsin 1, which contains both a well-folded N-terminal domain (ENTH), and a large, intrinsically disordered domain (Fig. 6A) (Busch et al., 2015; Kalthoff, Alves, Urbanke, Knorr, & Ungewickell, 2002), we observed the appearance of a high curvature vesicle population at lower concentration of full-length Epsin 1 in comparison to the isolated ENTH domain (Fig. 6B). This finding was in agreement with results from SUPER templates (Fig. 1B), which showed that full-length Epsin 1 drove greater membrane release than the ENTH domain alone. Collectively, these results suggest that the disordered domain, which occupies a large membrane footprint (Busch et al., 2015), enabled the full-length protein to reach a crowded environment with fewer membranebound protein copies compared to the smaller ENTH domain. Our tethered vesicle assay facilitated this important observation, and helped to elucidate a new paradigm for membrane fission in which bulky, disordered proteins may be among the most potent drivers of fission. While the procedures described here focus primarily on study of the Epsin 1 protein, this assay can be readily adapted to study other fission-driving proteins. Ultimately, this assay may help elucidate new and interesting behaviors of essential fission proteins, improving our understanding of the molecular mechanisms responsible for fission.

ACKNOWLEDGMENTS

J.C.S. acknowledges funding from the National Institutes of Health (R01GM120549). W.T.S. acknowledges the support of a Ruth L. Kirschstein NRSA Predoctoral Fellowship from the National Institutes of Health (F31GM121013), as well as a fellowship from the Graduate School at UT Austin.

REFERENCES

Aguet F, Antonescu C, Mettlen M, Schmid S, & Danuser G (2013). Advances in analysis of low signal-to-noise images link dynamin and AP2 to the functions of an endocytic checkpoint. Developmental Cell, 26(3), 279–291. [PubMed: 23891661]

Antonny B, Burd C, De Camilli P, Chen E, Daumke O, Faelber K, et al. (2016). Membrane fission by dynamin: What we know and what we need to know. The EMBO Journal, 35(21), 2270–2284. [PubMed: 27670760]

Boucrot E, Pick A, Camdere G, Liska N, Evergren E, McMahon H, et al. (2012). Membrane fission is promoted by insertion of amphipathic helices and is restricted by crescent BAR domains. Cell, 149(1), 124–136. [PubMed: 22464325]

Busch D, Houser J, Hayden C, Sherman M, Lafer E, & Stachowiak J (2015). Intrinsically disordered proteins drive membrane curvature. Nature Communications, 6, 7875.

Conner S, & Schmid S (2003). Regulated portals of entry into the cell. Nature, 422(6927), 37–44. [PubMed: 12621426]

Ellenbroek W, Wang Y, Christian D, Discher D, Janmey P, & Liu A (2011). Divalent cation-dependent formation of electrostatic PIP2 clusters in lipid monolayers. Biophysical Journal, 101(9), 2178–2184. [PubMed: 22067156]

Ford M, Mills I, Peter B, Vallis Y, Praefcke G, Evans P, et al. (2002). Curvature of clathrin-coated pits driven by epsin. Nature, 419(6905), 361–366. [PubMed: 12353027]

Franken L, Boekema E, & Stuart M (2017). Transmission electron microscopy as a tool for the characterization of soft materials: Application and interpretation. Advanced Science, 4(5), 1600476. [PubMed: 28546914]

Hatzakis N, Bhatia V, Larsen J, Madsen K, Bolinger P, Kunding A, et al. (2009). How curved membranes recruit amphipathic helices and protein anchoring motifs. Nature Chemical Biology, 5(11), 835–841. [PubMed: 19749743]

Helfrich W (1973). Elastic properties of lipid bilayers—Theory and possible experiments. Zeitschrift Fur Naturforschung C, 28(11), 693–703.

Hofmann H, Soranno A, Borgia A, Gast K, Nettels D, & Schuler B (2012). Polymer scaling laws of unfolded and intrinsically disordered proteins quantified with single-molecule spectroscopy. Proceedings of the National Academy of Sciences of the United States of America, 109(40), 16155–16160. [PubMed: 22984159]

Hoppins S, Lackner L, & Nunnari J (2007). The machines that divide and fuse mitochondria. Annual Review of Biochemistry, 76, 751–780.

Hurley J, Boura E, Carlson L, & Rozycki B (2010). Membrane budding. Cell, 143(6), 875–887. [PubMed: 21145455]

Jarsch I, Daste F, & Gallop J (2016). Membrane curvature in cell biology: An integration of molecular mechanisms. Journal of Cell Biology, 214(4), 375–387. [PubMed: 27528656]

Kalthoff C, Alves J, Urbanke C, Knorr R, & Ungewickell E (2002). Unusual structural organization of the endocytic proteins AP180 and epsin 1. Journal of Biological Chemistry, 277(10), 8209–8216. [PubMed: 11756460]

Kunding A, Mortensen M, Christensen S, & Stamou D (2008). A fluorescence-based technique to construct size distributions from single-object measurements: Application to the extrusion of lipid vesicles. Biophysical Journal, 95(3), 1176–1188. [PubMed: 18424503]

Lohr C, Kunding A, Bhatia V, & Stamou D (2009). Constructing size distributions of liposomes from single-object fluorescence measurements. Methods in Enzymology Liposomes, 465, 143–160. Pt. G.

McMahon H, & Gallop J (2005). Membrane curvature and mechanisms of dynamic cell membrane remodelling. Nature, 438(7068), 590–596. [PubMed: 16319878]

Mierzwa B, & Gerlich D (2014). Cytokinetic abscission: Molecular mechanisms and temporal control. Developmental Cell, 31(5), 525–538. [PubMed: 25490264]

Momin N, Lee S, Gadok A, Busch D, Bachand G, Hayden C, et al. (2015). Designing lipids for selective partitioning into liquid ordered membrane domains. Soft Matter, 11(16), 3241–3250. [PubMed: 25772372]

Neumann S, Pucadyil T, & Schmid S (2013). Analyzing membrane remodeling and fission using supported bilayers with excess membrane reservoir. Nature Protocols, 8(1), 213–222. [PubMed: 23288321]

Prevost C, Tsai F, Bassereau P, & Simunovic M (2017). Pulling membrane nanotubes from giant unilamellar vesicles. Journal of Visualized Experiments, 130, e56086.

Pucadyil T, & Schmid S (2008). Real-time visualization of dynamin-catalyzed membrane fission and vesicle release. Cell, 135(7), 1263–1275. [PubMed: 19084268]

Schoneberg J, Lee I, Iwasa J, & Hurley J (2017). Reverse-topology membrane scission by the ESCRT proteins. Nature Reviews Molecular Cell Biology, 18(1), 5–17. [PubMed: 27703243]

Snead W, Hayden C, Gadok A, Zhao C, Lafer E, Rangamani P, et al. (2017). Membrane fission by protein crowding. Proceedings of the National Academy of Sciences of the United States of America, 114(16), E3258–E3267. [PubMed: 28373566]

Stachowiak J, Schmid E, Ryan C, Ann H, Sasaki D, Sherman M, et al. (2012). Membrane bending by protein-protein crowding. Nature Cell Biology, 14(9), 944–949. [PubMed: 22902598]

Stewart J (1980). Colorimetric determination of phospholipids with ammonium ferrothiocyanate. Analytical Biochemistry, 104(1), 10–14. [PubMed: 6892980]

Takayama M, Itoh S, Nagasaki T, & Tanimizu I (1977). A new enzymatic method for determination of serum choline-containing phospholipids. Clinica Chimica Acta, 79(1), 93–98.

Zimmerberg J, & Kozlov M (2006). How proteins produce cellular membrane curvature. Nature Reviews Molecular Cell Biology, 7(1), 9–19. [PubMed: 16365634]

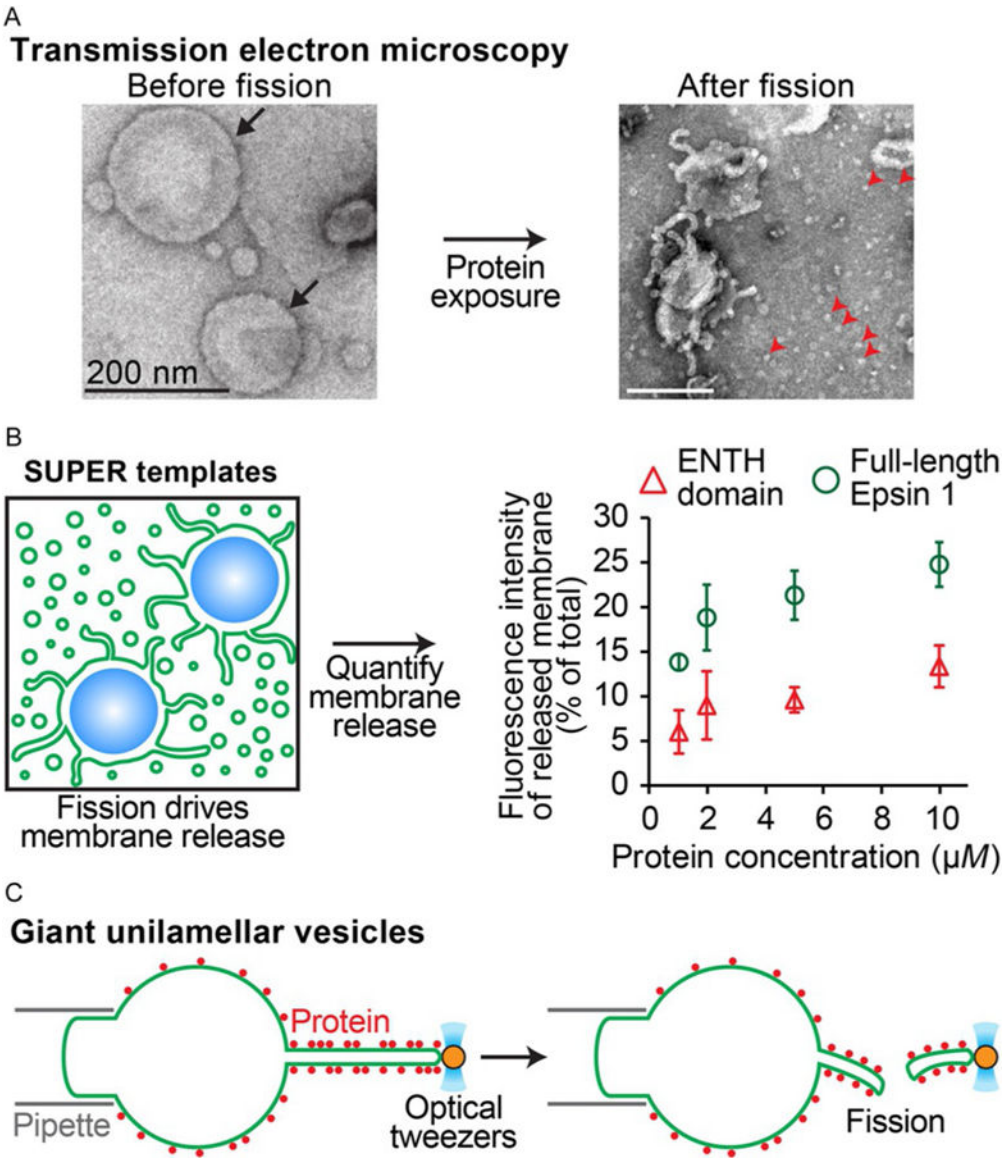

Fig. 1.

Some existing assays of membrane fission. (A) Negative stain transmission electron microscopy allows direct visualization of vesicles before (*left*) and after (*right*) exposure to fission-driving proteins. Highly curved vesicles (*red arrowheads*) are generated from the initially low-curvature vesicles (*black arrows*). Vesicle diameters must be measured manually. (B) SUPER templates, which are glass beads coated in low-tension membrane, undergo membrane release upon exposure to fission-driving proteins. Fission is quantified as the bulk fluorescence of the released membrane in the supernatant after sedimenting the beads. An example plot of membrane release is shown on the *right*. Full-length Epsin 1 drives greater membrane release compared to the Epsin 1 N-terminal homology (ENTH) domain alone, owing to enhanced crowding by the bulky disordered domain of full-length Epsin 1. SUPER template membrane-release experiments do not allow precise quantification of vesicle curvatures. (C) Pulling membrane nanotubes from giant unilamellar vesicles using

optical tweezers allows visualization of protein recruitment to high curvature membranes. Membrane tension is controlled via pipette aspiration of the vesicle, which provides control over the diameter of the pulled nanotube. Membrane fission results in tube breaking (*right*). These experiments are low-throughput, as only one vesicle and pulled tube can be examined at a time. *Images (panel A) and data (panel B) from the same experiments reported in Snead, W., Hayden, C., Gadok, A., Zhao, C., Lafer, E., Rangamani, P., et al. (2017). Membrane fission by protein crowding*. Proceedings of the National Academy of Sciences of the United States of America, 114*(16), E3258–E3267.*

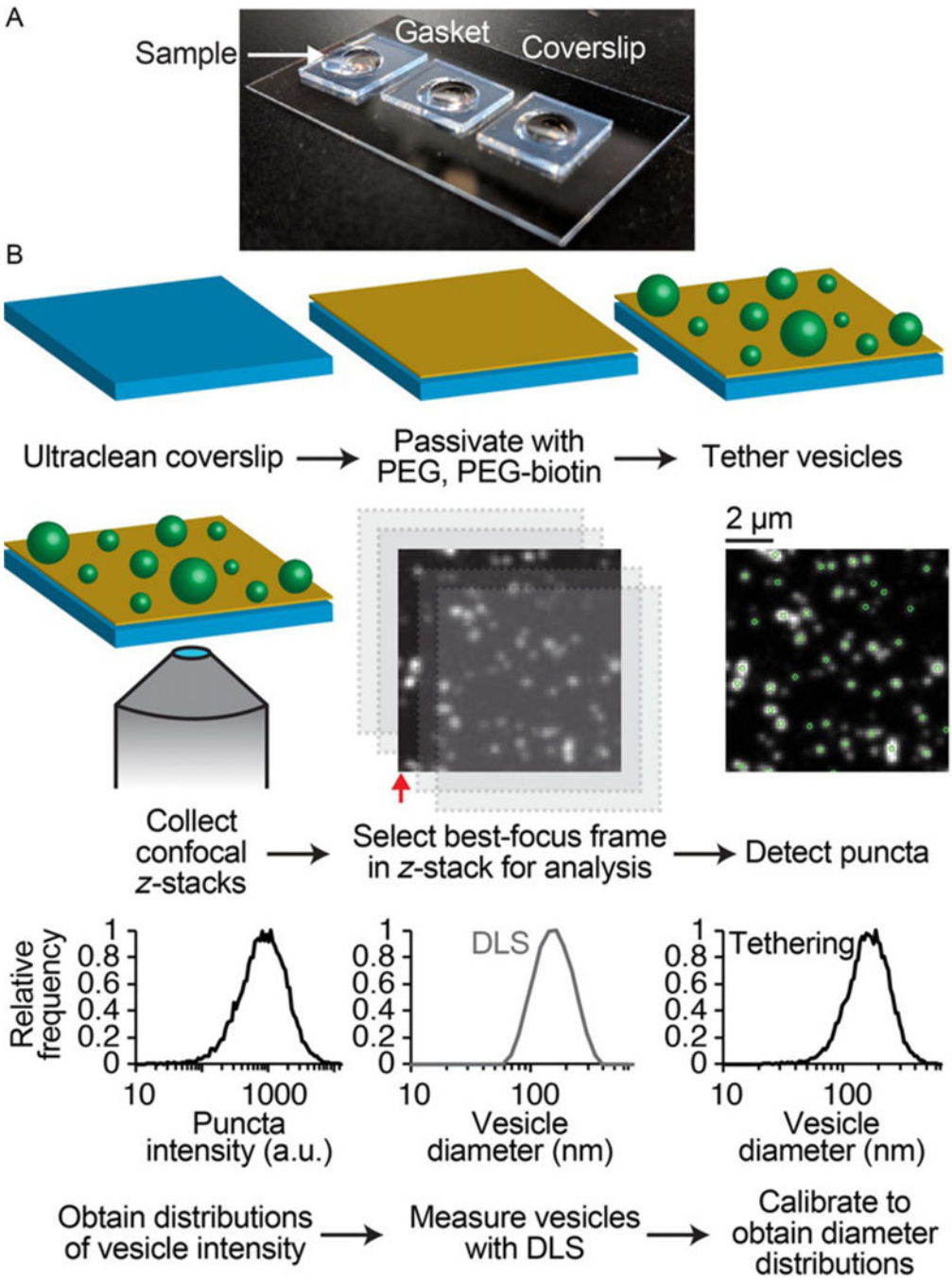

Fig. 2.

Tethered vesicle assay of membrane fission. (A) Photo of three sample wells on an ultraclean coverslip. The gaskets were made from silicone sheets, and will hold 40μL (see Section 2.2 for well preparation). (B) Workflow of tethered vesicle assay and image analysis to obtain distributions of vesicle diameter. This procedure is performed for a protein-free vesicle control, and the scaling factor calculated from calibration is used to generate vesicle diameter distributions for the fission samples.

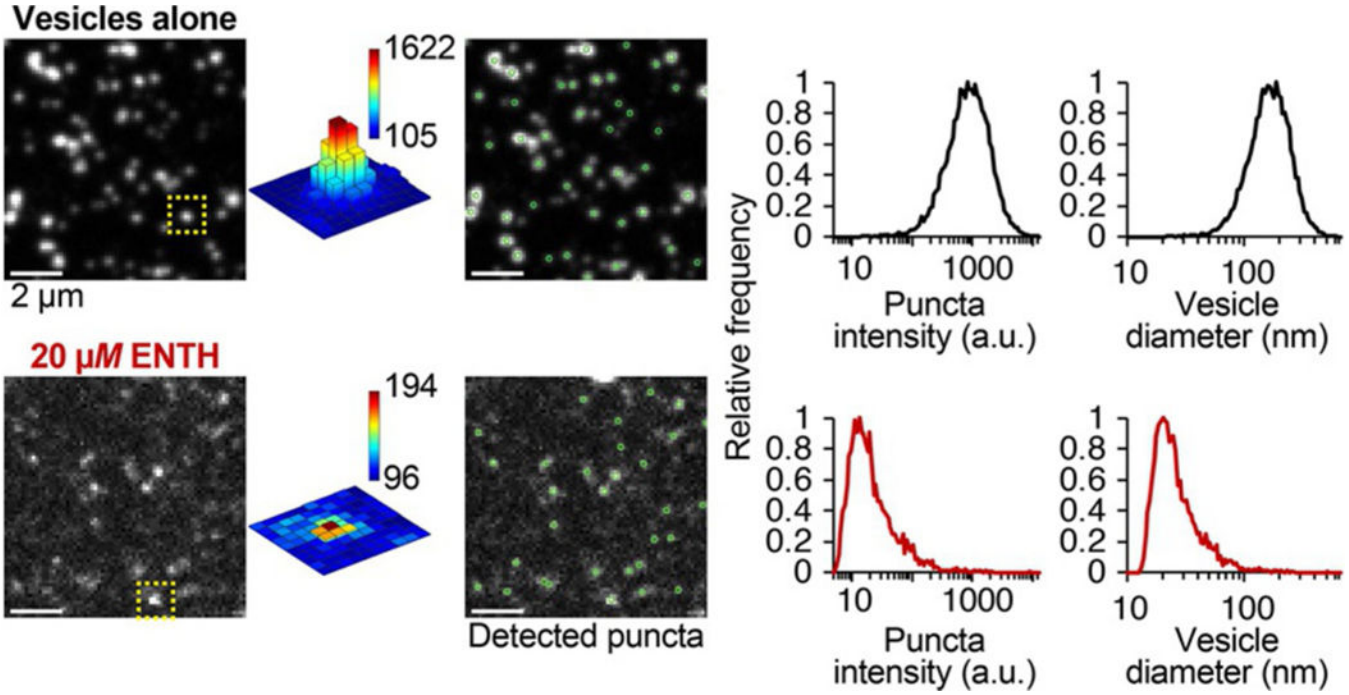

Fig. 3.

Tethered vesicle assay reveals potent membrane fission by the ENTH domain. *Top row*: Before protein exposure. *Bottom row*: After exposure to 20μ*M* ENTH. Contrast settings in the *top* and *bottom images* are different to show puncta clearly. The intensities of vesicle puncta are reduced after protein exposure, indicating fission. The *boxed region* in each image indicates vesicle intensity profile to the *right*, where the bar heights in both plots are scaled between 90 and 1622 brightness units and the *color map* corresponds to the specified range. The same images are shown again with the detected puncta from cmeAnalysis marked. The puncta intensity distributions indicate a strong reduction in vesicle intensity after protein exposure. The corresponding vesicle diameter distributions after calibration (*far right*) reveal a shift to a high curvature vesicle population after fission by ENTH. Scale bars: 2μm. *Data from the same experiments reported in Snead, W., Hayden, C., Gadok, A., Zhao, C., Lafer, E., Rangamani, P., et al. (2017). Membrane fission by protein crowding.* Proceedings of the National Academy of Sciences of the United States of America, 114*(16), E3258–E3267.*

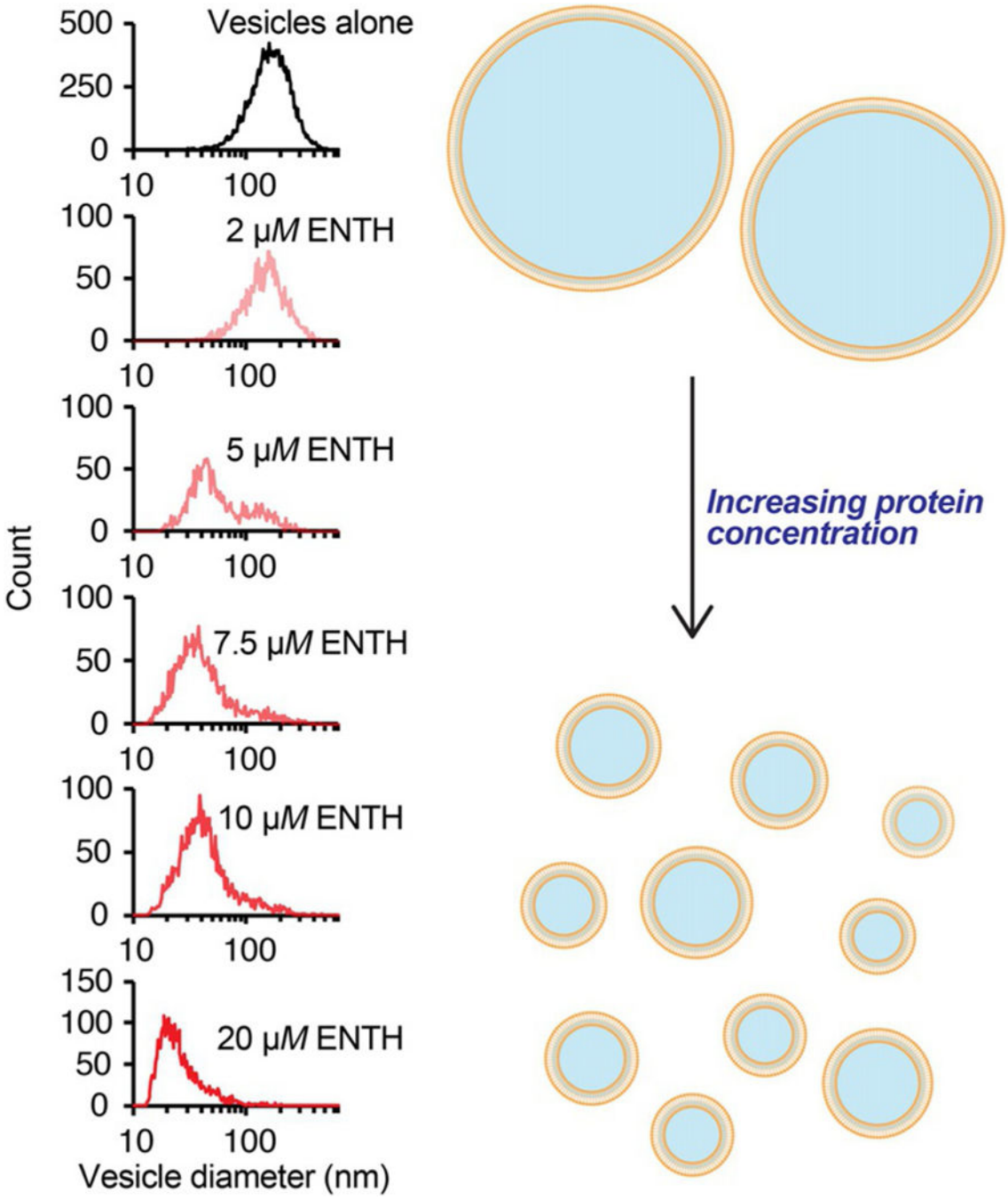

Fig. 4.

Progressive reduction in vesicle diameter revealed by tethered vesicle assay. *Left*: Histograms of vesicle diameter after exposure to the indicated concentrations of ENTH. *Right*: Vesicles are refined to progressively higher curvature populations as the concentration of protein increases. *Data from the same experiments reported in Snead, W., Hayden, C., Gadok, A., Zhao, C., Lafer, E., Rangamani, P., et al. (2017). Membrane fission by protein crowding.* Proceedings of the National Academy of Sciences of the United States of America, 114*(16), E3258–E3267.*

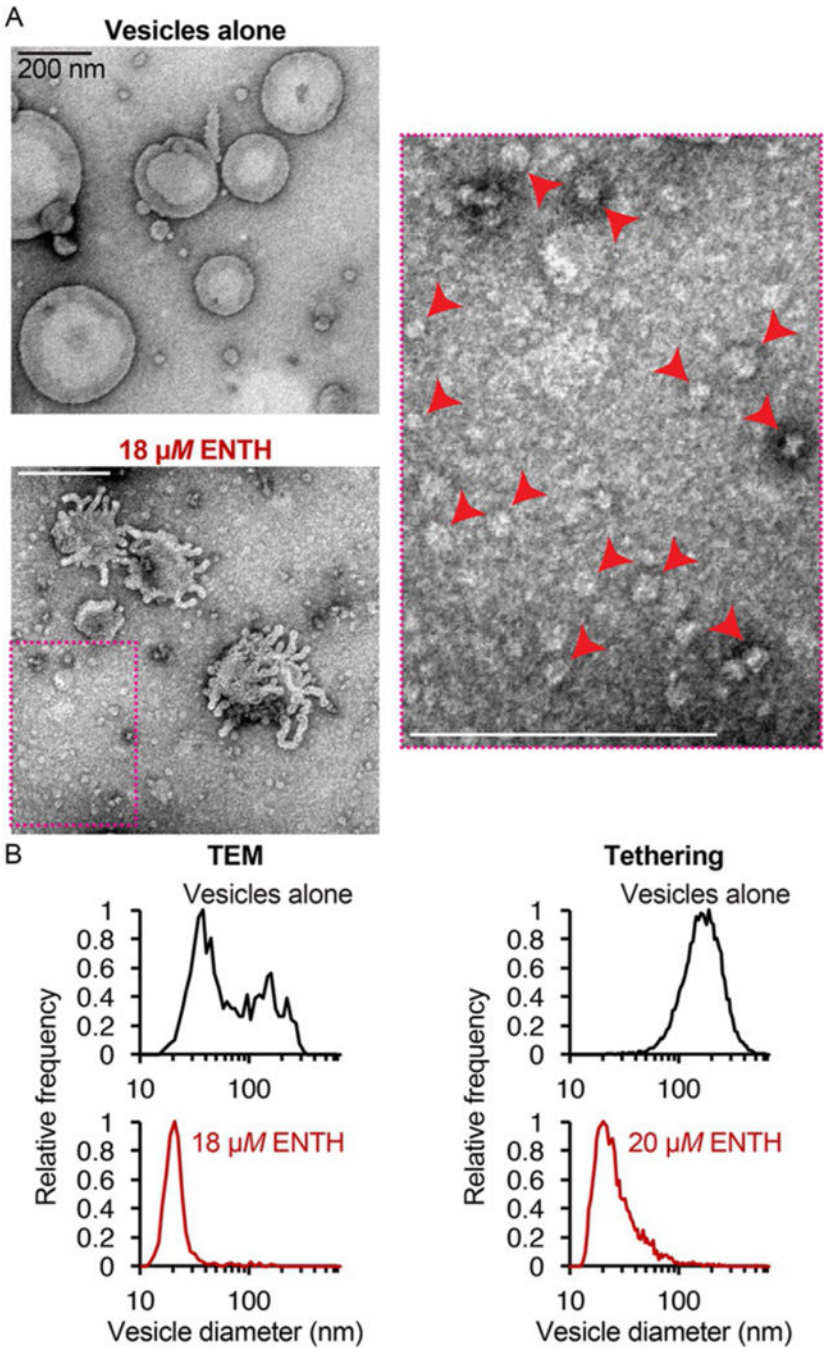

Fig. 5.

Comparison of tethered vesicle assay with transmission electron microscopy (TEM). (A) Electron micrographs of vesicles before protein exposure (*top*) and after exposure to 18μ*M* ENTH (*bottom*). Vesicles were adsorbed onto glow-discharged, carbon-coated TEM grids and stained with 2% uranyl acetate before imaging. *Dashed magenta box* indicates zoomed region to the *right. Red arrowheads* indicate high curvature fission products. Scale bars: 200nm. (B) Distributions of vesicle diameter before protein exposure (*top*) and after exposure to ENTH (*bottom*) as quantified from TEM images (*left*) and the tethered vesicle

assay (*right*). *Data from the same experiments reported in Snead, W., Hayden, C., Gadok, A., Zhao, C., Lafer, E., Rangamani, P., et al. (2017). Membrane fission by protein crowding.* Proceedings of the National Academy of Sciences of the United States of America, 114*(16), E3258–E3267.*

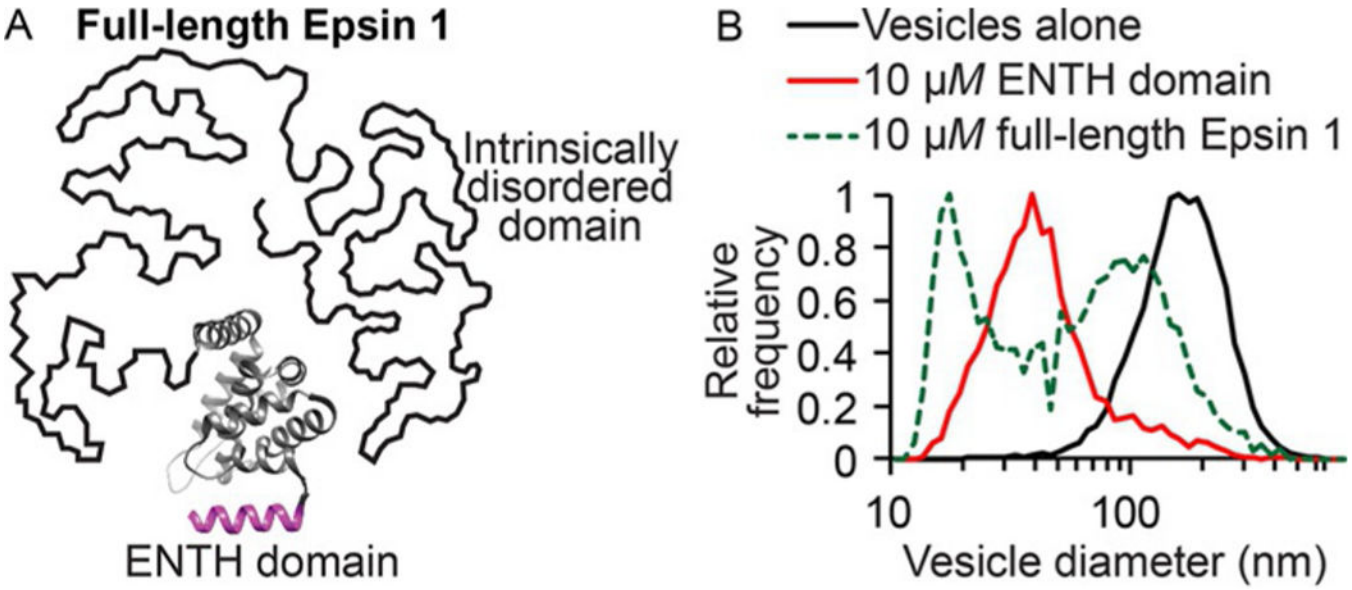

Fig. 6.

The intrinsically disordered domain of Epsin 1 enhances membrane fission by the ENTH domain. (A) Schematic of full-length Epsin 1, which contains a large, intrinsically disordered domain and the folded ENTH domain (PDB 1H0A). Full-length Epsin 1 occupies a significantly larger projected area on the membrane surface compared to the ENTH domain alone, thereby enabling full-length Epsin 1 to reach a crowded coverage of the membrane surface with fewer membrane-bound protein copies compared to ENTH. (B) Tethered vesicle assay reveals that at the same concentration, full-length Epsin 1 generates a high curvature fission vesicle population not observed with the isolated ENTH domain. *Data from the same experiments reported in Snead, W., Hayden, C., Gadok, A., Zhao, C., Lafer, E., Rangamani, P., et al. (2017). Membrane fission by protein crowding*. Proceedings of the National Academy of Sciences of the United States of America, 114*(16), E3258–E3267.*